

ÖSSZEFOGLALÓ

Ennek a munkának a célja olyan fotoakusztikus rendszer tervezése és építése, amely egyszerre képes mérni a $^{14}\text{NH}_3$ és a $^{15}\text{NH}_3$ ammónia izotópok koncentrációját. További cél az volt, hogy a rendszer robusztus, könnyen használható és automatizált legyen. A bemutatott fotoakusztikus (PA) mérőrendszer DFB dióda lézert használt fényforrásként, amelynek hullámhossza 1532 nm volt, és a hangolási tartomány körülbelül $\pm 1\text{nm}$. Ebben a tartományban mind a $^{14}\text{NH}_3$, mind a $^{15}\text{NH}_3$ erős abszorpciós vonalakkal rendelkezik. A kifejlesztett fotoakusztikus rendszerrel elért legkisebb kimutatható koncentráció (ami a mérési zaj háromszorosának felel meg) 0,278 ppm $^{14}\text{NH}_3$ és 1,661 ppm $^{15}\text{NH}_3$ esetén. A kifejlesztett PA rendszer elég kompakt és robusztus mind laboratóriumi, mind terepi alkalmazásokhoz.

Kulcsszavak: ammónia izotópok, fotoakusztikus spektroszkópia, elosztott visszacsatolású diódalézer

ABSTRACT

This work aims to design and build a photoacoustic system capable of detecting and measuring ammonia isotopes $^{14}\text{NH}_3$ and $^{15}\text{NH}_3$. A further aim is to ensure robustness ease of use and automatic operation. The photoacoustic measuring system uses a telecommunication type near-infrared DFB diode laser as a light source whose wavelength is 1532 nm, and the tuning range is approximately $\pm 1\text{nm}$. In this range, both $^{14}\text{NH}_3$ and $^{15}\text{NH}_3$ have strong absorption lines. The minimum detectable concentration (corresponding to the three times of the measurement noise) of the developed photoacoustic system is 0.278 ppm and 1.661 ppm for $^{14}\text{NH}_3$ and $^{15}\text{NH}_3$, respectively. The developed PA system is compact and robust enough for both laboratory and field applications.

Keywords; Ammonia Isotopes, Photoacoustic Spectroscopy, Distributed Feedback Diode laser



EMILY AWUOR*
HELGA HUSZÁR
ZOLTÁN BOZÓKI

Department of Optics and Quantum
Electronics, University of Szeged,
Hungary

*Corresponding Author, email:
mlawuor252@gmail.com

MEASUREMENT OF AMMONIA ISOTOPES ($^{14}\text{NH}_3$ AND $^{15}\text{NH}_3$) USING PHOTOACOUSTIC METHOD

*Az ammónia izotóp ($^{14}\text{NH}_3$ and $^{15}\text{NH}_3$) mérése
fotoakusztikus módszerrel*

*Merenje izotopa amonijaka ($^{14}\text{NH}_3$ and $^{15}\text{NH}_3$)
fotoakusztičnom metodom*

Introduction

Isotopes have been previously used in various scientific studies. Few examples include food forensics where it is used to trace the geographical origin of food (Korenaga, Suzuki, & Chikaraishi, 2019) and also in the assessment of diet and nutrition patterns among the human population (Katzenberg, 2008). In archaeology, isotopes have been applied to determine the mechanisms of evolution and immigration patterns (Reitsema, 2015), whereas, in criminology studies, isotopes have been used to classify and study seized illegal drugs, synthetic stimulants, explosives, food fraud and poisoning (Font et al., 2015), (Hurley, West, & Ehleringer, 2010). Some isotope applications in the environmental forensics science include fingerprinting of hydrocarbon fuel contaminants (Alimi, Ertel, & Schug, 2003), evaluation of transformation processes of general micropollutants in groundwater (Spahr et al., 2013), herbicide pollution (Elsayed et al., 2014), pharmaceutical pollution (Ketolainen et al., 1995), and consumer care products (Elsner & Imfeld, 2016), among others. In atmospheric science $\delta^{15}\text{N}$ and $\delta^{13}\text{C}$ have been previously used as indicators of climate and in the analysis of atmospheric pollution tracer studies.

Ammonia (NH_3) which has a characteristically pungent odour serves as a precursor to fertilizers and foodstuffs thereby making a major contribution to the nutritional needs of terrestrial organisms. Another use of NH_3 is in its function as a building block for the synthesis of several important pharmaceuticals. On the other hand, NH_3 has also been classified as a hazardous substance and a pollutant. Its natural occurrence in the atmosphere is in trace amounts but due to anthropogenic sources, these levels have greatly risen.

Currently, several methods have been employed for NH_3 measurements. These include; Flux measurement method e.g. Tracer Gas Ratio Technique (TGRT), enclosure & micro-meteorological methods and Passive Flux Samples (PFS). The main disadvantages of this method are high costs, replicability issues and difficulties in correctly duplicating surface and environmental aspects in closed spaces thereby leading to large approximations and empiricism (Harper, 2005). Out of the four techniques, only two namely TGRT and PFS have been confirmed to be applicable in NH_3 isotope measurements. The second method is the wet chemical sampling method which comprises of Saraz method for determination of NH_3 emissions (SMDAE) (Alexander, Saraz, Gates, Paula, & Mendes, 2012), Gas washing (Harper, 2005), continuous annular denuder systems (AMANDA) (Harper, 2005), wet efficient diffusion denuder (WEDD) (Schwab et al., 2007), and Long Path Absorption Photometer (LOPAP). SMDAE has good accuracy, is easy to construct and transport but is based on diffusion to a reaction surface hence requires a longer sampling time (hours) (Alexander et al., 2012). Gas washing has high sensitivity but is labour intensive and prone to sample contamination hence is mostly applicable where fast sampling is not required. Amanda is most suitable for micro-meteorological gradient measurement of NH_3 but has a low precision (Harper, 2005). Apart from Amanda and WEDD, the other wet chemical sampling methods suitability to NH_3 isotope measurements has not been reported in the literature.

The most widely used NH_3 measurement method is spectrometry. Here several instruments/techniques have been applied. Examples are; Fourier Transform Infrared Spectrometry (FTIR) which is capable of simultaneous measurement of several gas species although in some instances it may have limited sensitivity due to spectral overlap. Chemical Ionization Mass Spectrometry (CIMS) which uses ion-molecule reactions to selectively ionise and detect trace NH_3 in ambient air, is sensitive, selective and offers reliably fast time resolution. CIMS major challenge is in the understanding and controlling of its background signal (Nowak et al., 2007). Ion Mobility Spectrometry (IMS) is based on the determination of the mobility in electric fields of gas-phase ions derived from constituents in a target sample. IMS has high sensitivity and fast response during ion mobility spectra but low resolving power and very limited selectivity (Borsdorf & Eiceman, 2006). Tunable Diode Laser Absorption Spectrometers (TDLAS) can achieve traceability in spectroscopic amounts without the need for calibration using gas standards but is highly sensitive to noise levels (Schwab et al., 2007). Chemiluminescence detectors have also been applied in NH_3 measurements. Although a simple instrument with low detection limits and wide dynamic ranges, it suffers from a lack of sufficient selectivity and sensitivity to various physicochemical factors. Differential Optical Absorption Spectroscopy (DOAS) has a fast response and low maintenance but high noise levels. Quantum Cascade Laser Absorption Spectroscopy (QCLAS) has high sensitivity, fast response time and a high spectral resolution which gives good selectivity between different targeted species (Whitehead et al., 2008). Lastly and of importance to our work is the Photoacoustic Spectroscopy (PAS) which has been documented to be easy to operate under field conditions, have a high

precision and fast time response (Von Bobrutzki et al., 2010). Although most spectrometry methods can detect NH_3 isotopes, they are unable to distinguish between its isotopologues. This work seeks to use a locally fabricated photoacoustic cell to detect and measure the NH_3 gas isotopes concentration.

Instrumentation and Photoacoustic Detection Unit Set-Up

The measurement system consisted of the following main parts; a photoacoustic detection unit for concentration measurement, ammonia isotope gas generating unit, and gas handling as shown in Figures 1 and 2.

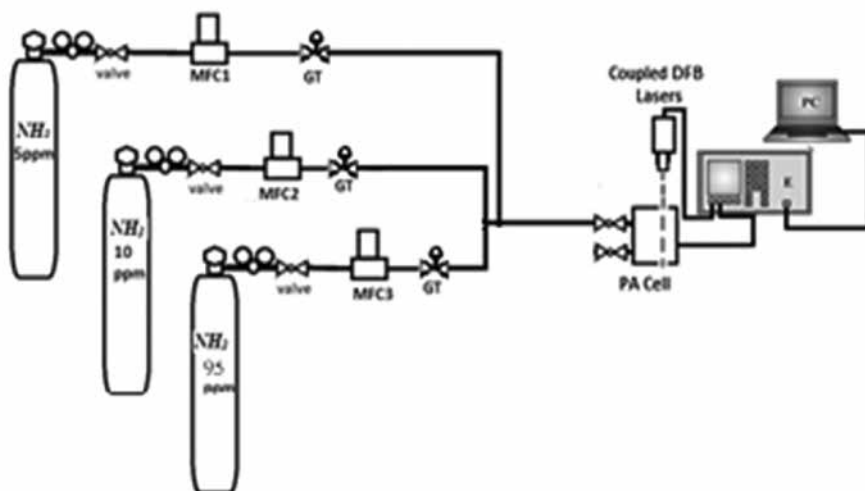


Figure 1; Schematic of the experimental setup for $^{14}\text{NH}_3$ calibration consisting of coupled DFB lasers connected to different concentrations of NH_3 gas cylinders, mass flow controllers (MFC), gas tap (GT), a photoacoustic signal analyzer (E = electronics) and a storage unit (personal computer, PC).

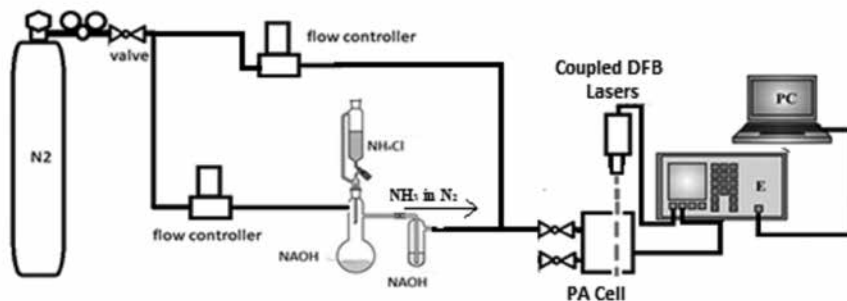


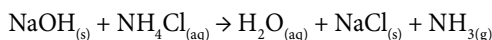
Figure 2; Schematic of the experimental setup for the $^{15}\text{NH}_3$ calibration consisting of coupled DFB lasers connected to the NH_3 gas generating system, a photoacoustic signal analyzer (E = electronics), and a storage unit (personal computer, PC).

In both Figures 1 and 2, the telecommunication type fibre coupled Distributed Feedback (DFB) diode lasers used are manufactured by Furukawa Inc. (FOL15DCWD-A82-19570- A), and its light power is approximately 45 mW. The laser coupler used is from Fiberlogix (FL-PBC-64-P-2-L-1-Q), and the measured combined laser light power is about 80 mW (due to some coupling losses) at the maximum allowable driving current ($I_{\text{max}} = 300 \text{ mA}$), and an emission wavelength of 1532 nm with a tuning range of $\pm 1 \text{ nm}$. The spectrum recording time was approximately 60 minutes. Recorded between 8-30 °C with 0.05 °C steps, with wavelength modulation whereby both laser wavelength and intensity are modulated by the application of a sine wave signal through an injection current. This allows a shift of the detection bandwidth to higher frequencies where there is an efficient laser intensity noise reduction resulting in a high sensitivity detection.

The electronics labelled as E in both Figures. 1 and 2, was an integrated unit from VIDEOTON Holding Plc., Hungary used to generate and feed the modulated current to the diode laser and also control the laser temperature. The electronic unit was also used for averaging and processing the generated PA signal (microphone signal), by providing an electrical amplification and quantifying the NH_3 concentration from the recorded signal by use of the digital lock-in technique. The unit also has an RS232 / RS485 interface which allows a real-time mode measurement of the NH_3 concentration to be transferred to an attached personal computer labelled PC in Fig.1. Lastly, it is equipped with a short term memory that enables the storage of measured data for up to two months.

Ammonia Gas Generation

The reaction below was used in the generation of NH_3 gas;

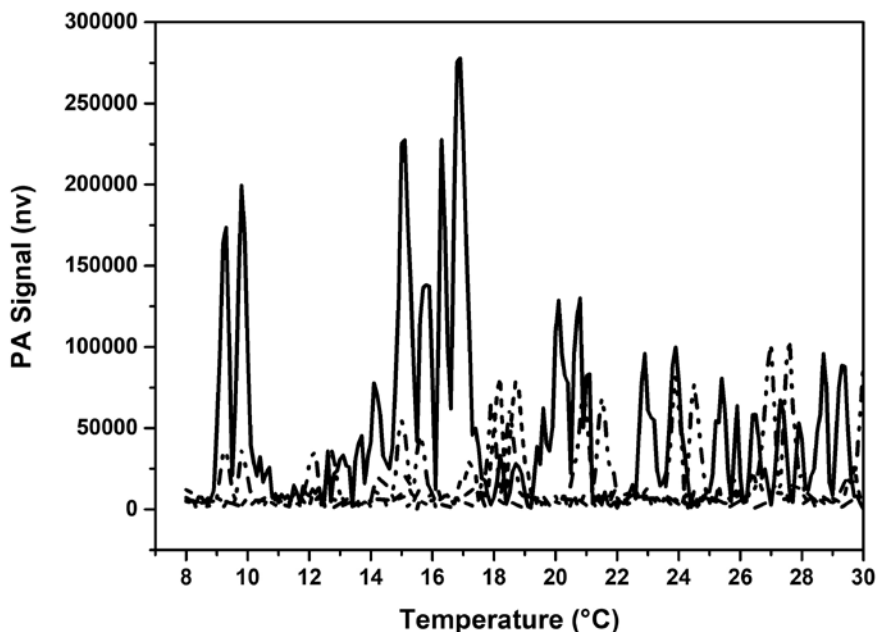


Granular NaOH and two types of ammonium chloride were used; ammonium- ^{15}N chloride (Sigma Aldrich ≥ 98 atom % $^{15}\text{N} \geq 99\%$) and normal ammonium chloride (Sigma Aldrich $\geq 99,5\%$). A side-tubed Erlenmeyer flask was fitted with gas inlet pipes on both sides and solid NaOH (0.1g) put in the flask. One side tube was introduced with 5.0 pure N_2 gas, which was used as a diluent and carrier gas, at a flow rate of 100 ml/min. On the other tube, the developed mixture of NH_3 and N_2 was exited. NH_4Cl (0.14g) dissolved in 10 ml of distilled water for 20-25 minutes was added to the flask via a dropping funnel from above as shown in figure 2. The developed NH_3 - N_2 gas mixture was then passed over granular NaOH for drying and into the PA cell for a spectrum recording. According to our calculations, 5000 ppm ammonia was generated.

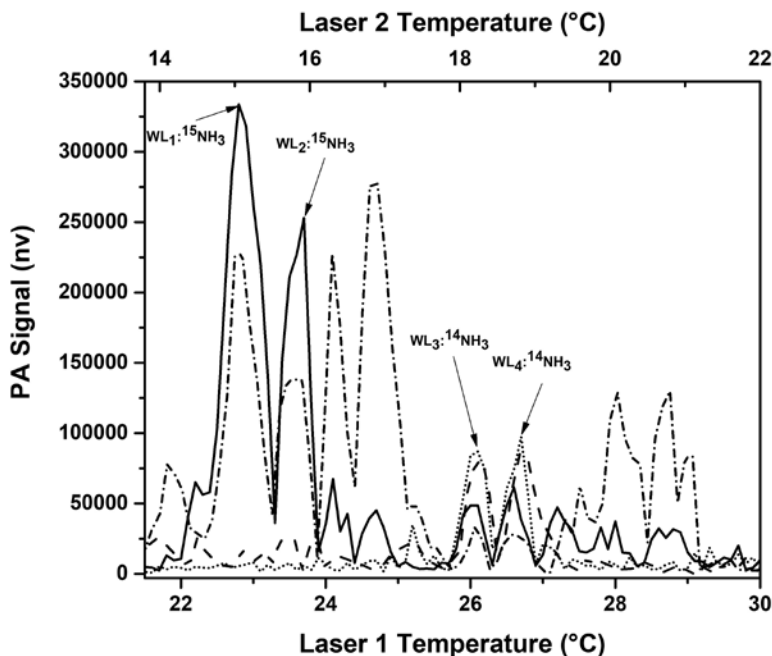
First, $^{14}\text{NH}_3$ and $^{15}\text{NH}_3$ spectra were recorded using two DFB diode lasers separately, with the same modulation parameters. The wavelength modulation (WM) was used during the measurements due to its improved sensitivity and noise-rejection capabilities over amplitude modulation, the WM spectrum is a derivative form of the absorption spectrum. The AC/DC values used were 10mA /146.5mA respectively and the N_2 flow rate was set to 100 sccm for the first 20 minutes to enable the measurement to stabilize, after which the cell was locked. Then, the measurement wavelength and PA signal calculation methods were selected, after which the calibration parameters were determined by fitting a calibration line to the data points shown in the graph, where the x and y coordinates are the isotope concentration and the corresponding calculated PA signal. The slope of the calibration line in nV/ppm corresponds to the sensitivity of the NIR-PA system. The minimum detectable concentration of both isotopes was calculated by dividing three times the noise of the PA measurement by the sensitivity associated with the corresponding isotopes. Calibration of $^{14}\text{NH}_3$ was done using 5ppm, 10ppm, 95ppm NH_3 gas cylinders while, $^{15}\text{NH}_3$ calibration was done using the provided solutions of $^{15}\text{NH}_3$: $^{14}\text{NH}_3$ (0%: 100%), $^{15}\text{NH}_3$: $^{14}\text{NH}_3$ (25%: 75%), $^{15}\text{NH}_3$: $^{14}\text{NH}_3$ (50%: 50%), $^{15}\text{NH}_3$: $^{14}\text{NH}_3$ (75%: 25%) & $^{15}\text{NH}_3$: $^{14}\text{NH}_3$ (100%: 0%). Each of all the concentrations was measured for about one hour in closed mode. After each measurement, the cell was purged with pure N_2 gas before switching the solutions. (Huszár et al., 2008), reported that for NH_3 gas detection, cross-sensitivity with CO_2 and water vapour gases is a major challenge and that this tends to occur at specific wavelength ranges. In our measurements, the cross-sensitivity of the developed system was checked by spectra of 100% CO_2 and water vapour buffered in N_2 gas (the water vapour concentration about 5%).

Results and Discussion

Graph 1 below shows a comparison measurement of ammonia isotopes, water vapour and carbon dioxide since their wavelength coincide. In addition to the modulation parameters used, it can be seen that water vapour does not cause any cross-sensitivity. The maximum CO_2 signal is 100000nV, then the normal air contains 400 ppm CO_2 , the signal is 40nV, this signal causes negligible cross-sensitivity.



Graph 1: Comparison of cross-sensitivity spectra of different measured components, 5% water vapour (dash line), 100 % CO_2 (dash dot line), 95ppm $^{14}\text{NH}_3$ (dot line), 600 ppm $^{15}\text{NH}_3$ (solid line).

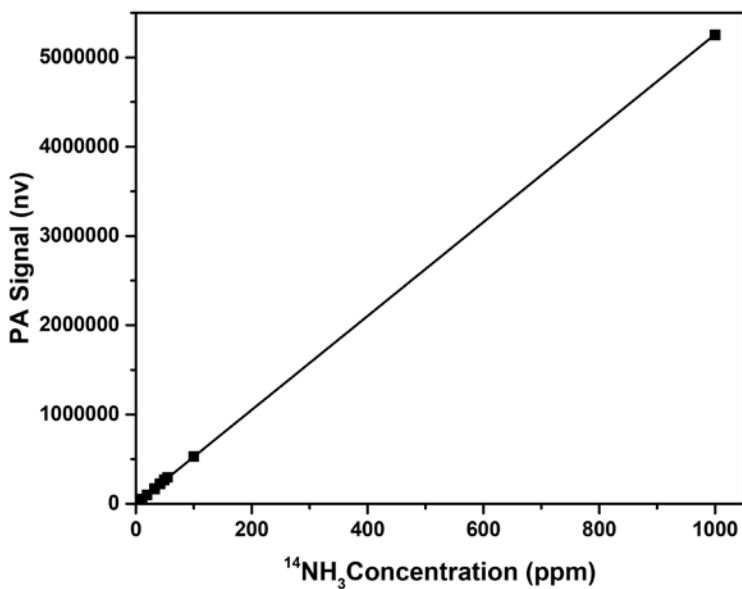


Graph 2: Selection of wavelength for measurement of $^{14}\text{NH}_3$ and $^{15}\text{NH}_3$ by recorded spectra. The upper X-axis corresponds to the temperature of Laser 2, depicting $^{14}\text{NH}_3$ (dot line) and $^{15}\text{NH}_3$ (dash-dot line) while the lower X-axis corresponds to the temperature of Laser 1, depicting $^{14}\text{NH}_3$ (dash line) and $^{15}\text{NH}_3$ (solid line).

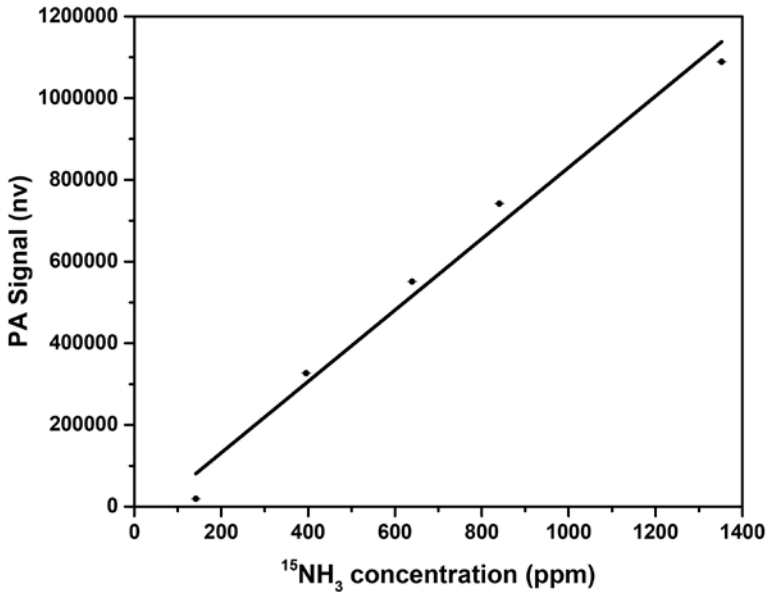
Graph 2. Shows four chosen wavelengths for the $^{14}\text{NH}_3$ and $^{15}\text{NH}_3$ calibration measurements. Two wavelengths for $^{14}\text{NH}_3$, two wavelengths for $^{15}\text{NH}_3$ measurements. To determine the $^{14}\text{NH}_3$ and $^{15}\text{NH}_3$ concentrations, the difference between the PA signals measured at two-two wavelengths corresponds to the $^{14}\text{NH}_3$ and $^{15}\text{NH}_3$ concentrations. This concentration calculation is based on the fact that PA signals have opposite phases at these two absorption maxima. For $^{15}\text{NH}_3$ concentrations calculation difference between the PA signals measured at WL1 and WL2 were used. For $^{14}\text{NH}_3$ concentrations calculation difference between the PA signals measured at WL3 and WL4 were used. The measuring temperatures were set as defined in the **Table 1**. The calibration curve thus obtained is as shown in Graph 3.

TABLE 1: Selection of temperatures used for the $^{14}\text{NH}_3$ and $^{15}\text{NH}_3$ calibrations.

LASER 1		LASER 2	
WL1	14.90 °C ; $^{15}\text{NH}_3$	WL1	22.70 °C ; $^{15}\text{NH}_3$
WL2	15.80 °C ; $^{15}\text{NH}_3$	WL2	23.50 °C ; $^{15}\text{NH}_3$
WL3	17.20 °C ; $^{14}\text{NH}_3$	WL3	25.10 °C ; $^{14}\text{NH}_3$
WL4	18.20 °C ; $^{14}\text{NH}_3$	WL4	26.00 °C ; $^{14}\text{NH}_3$



(a).



(b).

Graph 3: Calibration curve of (a) $^{14}\text{NH}_3$ at temperatures (WL3 + WL4) and (b) $^{15}\text{NH}_3$ at temperatures (WL1 + WL2) using different concentrations.

From the calibration curve of $^{14}\text{NH}_3$ concentration in the solution, we can determine the $^{15}\text{NH}_3$ (Graph 3b) concentration in the solution. From Graphs 3 (a & b), the sensitivity of the fabricated system and minimum detectable concentration on each peak temperature was calculated as follows;

$$\text{MDAC} = (3\sigma_{\text{max}})/S = (3 \cdot 483.34941) / 5257.7961 = 0.278 \text{ ppm}$$

$$\text{MDAC} = (3\sigma_{\text{max}})/S = (3 \cdot 483.34941) / 873.06433 = 1.661 \text{ ppm}$$

The detection limit from the two calibration curves for $^{14}\text{NH}_3$ and $^{15}\text{NH}_3$ was 0.278 ppm and 1.661 ppm (3 σ) respectively.

Conclusions

This work has shown that measurement of ammonia isotopes ($^{14}\text{NH}_3$ and $^{15}\text{NH}_3$) using a photoacoustic measuring system fitted with a wavelength-modulated, room temperature operated, telecommunication type near-infrared diode laser light source of wavelength 1532 nm is possible. Both NH_3 isotopes recorded strong absorption lines at this particular wavelength while the values of their minimum detectable concentrations were 0.278 ppm for $^{14}\text{NH}_3$ and 1.661 ppm for $^{15}\text{NH}_3$.

Acknowledgement

Emily Awuor wishes to acknowledge the Tempus Public Foundation for the award of the Stipendium Hungaricum Scholarship which enabled and provided the platform to be able to carry out this research. This work was supported by the NKFIH-1279-2/202 - Thematic Excellence Program of the Ministry for Innovation and Technology, Hungary. The authors also thank the financial support of the “GINOP-2.3.4-15-2020-00006” project.

References

- Alexander, J., Saraz, O., Gates, R. S., Paula, M. O. D. E., & Mendes, L. B. (2012). Evaluation of different methods for determining Ammonia emissions in poultry buildings and their applicability to open facilities. *DYNA. Magazine of the Faculty of Mines, National University of Colombia.*, 51–60.
- Alimi, H., Ertel, T., & Schug, B. (2003). Fingerprinting of Hydrocarbon Fuel Contaminants : Literature Review. *Environmental Forensics*, 4(June 2013), 25–38. <https://doi.org/10.1080/15275920390186949>
- Borsdorf, H., & Eiceman, G. A. (2006). Ion mobility spectrometry: Principles and applications. *Applied Spectroscopy Reviews*, 41(4), 323–375. <https://doi.org/10.1080/05704920600663469>
- Elsayed, O. F., Maillard, E., Vuilleumier, S., Nijenhuis, I., Richnow, H. H., & Imfeld, G. (2014). Using compound-specific isotope analysis to assess the degradation of chloroacetanilide herbicides in lab-scale wetlands. *Chemosphere*, 99, 89–95. <https://doi.org/10.1016/j.chemosphere.2013.10.027>
- Elsner, M., & Imfeld, G. (2016). Compound-specific isotope analysis (CSIA) of micropollutants in the environment - current developments and future challenges. *Current Opinion in Biotechnology*, 41, 60–72. <https://doi.org/10.1016/j.copbio.2016.04.014>
- Font, L., Van Der Peijl, G., Van Leuwen, C., Van Wetten, I., & Davies, G. R. (2015). Identification of the geographical place of origin of an unidentified individual by multi-isotope analysis. *Science and Justice*, 55(1), 34–42. <https://doi.org/10.1016/j.scijus.2014.06.011>
- Harper, L. A. (2005). Ammonia : Measurement Issues. In J. L. Hatfield & J. M. Baker (Eds.), *Agronomy Monographs* (pp. 345–379). <https://doi.org/https://doi.org/10.2134/agronmonogr47.c15>
- Hurley, J. M., West, J. B., & Ehleringer, J. R. (2010). Stable isotope models to predict geographic origin and cultivation conditions of marijuana. *Science and Justice*, 50(2), 86–93. <https://doi.org/10.1016/j.scijus.2009.11.003>
- Huszár, H., Pogány, A., Bozóki, Z., Mohácsi, Á., Horváth, L., & Szabó, G. (2008). Ammonia monitoring at ppb level using photoacoustic spectroscopy for environmental application. *Sensors and Actuators, B: Chemical*, 134(2), 1027–1033. <https://doi.org/10.1016/j.snb.2008.05.013>
- Katzenberg, M. A. (2008). Stable Isotope Analysis : A tool for studying past diet, demography, and life history. In M. A. Katzenberg & S. R. Saunders (Eds.), *Biological Anthropology of the Human Skeleton, Second Edition* (pp. 413–441). John Wiley & Sons, Inc.
- Ketolainen, J., Oksanen, M., Rantala, J., Stor-Pellinen, J., Luukkala, M., & Paronen, P. (1995). Photoacoustic evaluation of elasticity and integrity of pharmaceutical tablets. *International Journal of Pharmaceutics*, 125(1), 45–53. [https://doi.org/10.1016/0378-5173\(95\)00110-5](https://doi.org/10.1016/0378-5173(95)00110-5)

- Korenaga, T., Suzuki, Y., & Chikaraishi, Y. (2019). Biochemical Stable Isotope Analysis in Food Authenticity. In A. M. Grumezescu & A. M. Holban (Eds.), *Engineering tools in the beverage industry* (pp. 209–226). Woodhead Publishing.
- Nowak, J. B., Neuman, J. A., Kozai, K., Huey, L. G., Tanner, D. J., Holloway, J. S., ... Fehsenfeld, F. C. (2007). A chemical ionization mass spectrometry technique for airborne measurements of ammonia. *Journal of Geophysical Research Atmospheres*, 112(10), 1–12. <https://doi.org/10.1029/2006JD007589>
- Reitsema, L. J. (2015). Laboratory and field methods for stable isotope analysis in human biology. *American Journal of Human Biology*, 27(5), 593–604. <https://doi.org/10.1002/ajhb.22754>
- Schwab, J. J., Li, Y., Bae, M. S., Demerjian, K. L., Hou, J., Zhou, X., ... Pryor, S. C. (2007). A laboratory intercomparison of real-time gaseous ammonia measurement methods. *Environmental Science and Technology*, 41(24), 8412–8419. <https://doi.org/10.1021/es070354r>
- Spahr, S., Huntscha, S., Bolotin, J., Maier, M. P., Elsner, M., Hollender, J., & Hofstetter, T. B. (2013). Compound-specific isotope analysis of benzotriazole and its derivatives. *Analytical and Bioanalytical Chemistry*, 405(9), 2843–2856. <https://doi.org/10.1007/s00216-012-6526-1>
- Von Bobruzki, K., Braban, C. F., Famulari, D., Jones, S. K., Blackall, T., Smith, T. E. L., ... Nemitz, E. (2010). Field inter-comparison of eleven atmospheric ammonia measurement techniques. *Atmospheric Measurement Techniques*, 3(1), 91–112. <https://doi.org/10.5194/amt-3-91-2010>
- Whitehead, J. D., Twigg, M., Famulari, D., Nemitz, E., Sutton, M. A., Gallagher, M. W., & Fowler, D. (2008). Evaluation of laser absorption spectroscopic techniques for eddy covariance flux measurements of ammonia. *Environmental Science and Technology*, 42(6), 2041–2046. <https://doi.org/10.1021/es071596u>